# Implications of bi-directional interaction on seismic fragilities of structures

Debdulal Pramanik, Abhik Kumar Banerjee and Rana Roy[*]

*Department of Aerospace Engineering and Applied Mechanics, Indian Institute of Engineering Science and Technology, Shibpur (erstwhile Bengal Engineering and Science University, Shibpur), Howrah 711 103, India*

**Abstract.** Seismic structural fragility constitutes an important step for performance based seismic design. Lateral load-resisting structural members are often analyzed under one component base excitation, while the effect of bi-directional shaking is accounted per simplified rules. Fragility curves are constructed herein under real bi-directional excitation by a simple extension of the conventional Incremental Dynamic Analysis (IDA) under uni-directional shaking. Simple SODF systems, parametrically adjusted to different periods, are examined under a set of near-fault and far-fault excitations. Consideration of bi-directional interaction appears important for stiff systems. Further, the study indicates that the peak ground accelertaion, velocity and displacement (PGA, PGV and PGD) of accelerogram are relatively stable and efficient intensity measures for short, medium and long period systems respectively. '30%' combination rule seems to reasonably predict the fragility under bi-directional shaking at least for first mode dominated systems dealt herein up to a limit state of damage control.

**Keywords:** bi-directional; reinforced concrete; near-fault; far-fault; Incremental Dynamic Analysis (IDA); seismic structural fragility

## 1. Introduction

In the event of an earthquake, lateral load-resisting structural members are subjected to lateral excitation that involves three translational and three rotational components. While the influence of rotational components is presumed to be important in special cases (Kubo and Penzien 1979), the effect of vertical translational component of ground motion may often be small (Beyer and Bommer 2007). However, the simultaneous action of pair of horizontal components is known to induce potentially higher inelastic seismic demand in reinforced concrete (RC) element relative to the associated damage under uni-directional shaking. Observations of several shake table tests under bi-directional (Kitajima *et al.*1992, 1996, Nakayama *et al.* 1996, 2000, Hachem *et al.* 2003) excitation as well as the comprehensive computational work (Sengupta *et al*. 2016) confirms such additional vulnerability under bi-directional shaking. Common practice is to determine separately the peak responses of the structure that are due to each component of ground motion - with the horizontal components applied along the principal axes of structure and combine these peak

---

∗Corresponding author, Professor, E-mail: rroybec@yahoo.com

responses according to one of the multicomponent combination rules, such as 30%-rule (AASHTO 1998, IS: 1893 2002).

In this backdrop, it may be recalled that the estimation of the probabilities of exceeding certain demand associated with a limit state in terms of suitable ground motion intensity measure (IM) is a fundamental step for performance based seismic design (Moehle and Deierlein 2004). This is expressed by fragility curve which is often constructed using structural response at increasing IMs. Incremental dynamic analysis (IDA) is a popular tool for estimation of seismic demand of structures (Vamvatsikos 2002). Conventional IDA involves performing several nonlinear dynamic analyses of a structure using a suite of accelerogram. To capture dynamic behaviour of the structural system - ranging from elastic to global dynamic instability - each record is scaled to multiple levels of intensity and the structural response is evaluated at each IM. This results in a plot of structural demand as a function of the IM and this serves as a key input to construct fragility. In IDA, one-component seismic excitation is traditionally applied.

Selection of an effective is another engineering challenge. An effective IM is defined as the one that yields a relatively stable estimate of demand at a specific IM level. Studies (Ebrahimian *et al.* 2015) have been expended to evaluate the predictive capability of different alternative IMs. A good review of such studies is available in a recent work (Banerjee et al., 2016). However, the efficiency of the available IMs in the context of two-component shaking has hardly been examined.

The present investigation, therefore, aims to establish a rational yet straightforward extension of the conventional IDA under uni-directional shaking to account for the bi-directional interaction. Major concerns of intensifying two components simultaneously as well as appropriately selecting and representing IMs under two-component are discussed. Legitimacy and the choice of IMs are established by estimating seismic fragility under a suite of motions. Near-fault (NF) and far-fault (FF) motions are separately considered. The study is conducted with a single story building frame parametrically adjusted to different periods of vibration. Inter-storey drift is chosen as engineering demand parameter of interest. Present investigation appears useful to account for bi-directional shaking in seismic design.

## 2. Conventional IDA and fragility

Standard IDA involves subjecting the structure with increasing intensity till the intended demand is reached. The concept of IDA (Bertero 1977, Nassar and Krawinkler 1991), also termed dynamic pushover, has recently been used by Vamvatsikos and Cornell in several studies (2002a, b, 2004a, b, 2005). The conventional IDA procedure detailed elsewhere (Vamvatsikos 2002) fundamentally include the following:

• A set of ground motions, compatible with a design scenario, is scaled to multiple intensities and response of structure is evaluated at each level.

• Suitable demand parameter is plotted as a function of IM, i.e., IDA curve.

It is needless to mention that the resulting IDAs correspond to differences in estimated demand at a specified IM due to inherent randomness in the records employed. Thus the IDA results are usually interpreted in probabilistic format through fragility construction.

Considering different ground motion characteristics and the traditionally used IM, we assume different IMs. These IMs may be broadly categorized in terms of their dependency or independency with structural properties. While pseudo-spectral acceleration ($S_a$) belonging to first category is considered, the second category includes peak ground acceleration (PGA), velocity

(PGV), displacement (PGD) and Arias Intensity ($I_A$), Cumulative Absolute Velocity (CAV). It may be noted that PGA, PGV and PGD only represent instantaneous amplitudes of acceelrogram, whence $I_A$ and CAV are integral measures of ground motion characteristics. We have further considered *energetic length* ($L_e \approx a_g \times T_m^2$ where $a_g$ is PGA and $T_m$ represents mean period of motion defined in Rathje *et al.* 1998, 2004) of motion, independent of structural characteristics, in view of the inspiring performance of the parameter to establish order in seismic response (Roy *et al.* 2015, Chakroborty and Roy 2016).

To construct fragility curves, it is common to assume that the variation of IM values of ground motions corresponding to a specified demand of a given structure follows a lognormal distribution. This consideration is reasonable and confirmed by several researchers (Porter *et al.* 2007, Bradley and Dhakal 2008, Ghafory-Ashtiany *et al.* 2010, Eads *et al.* 2013, Banerjee *et al.* 2016). To define the fragility curve, a lognormal cumulative distribution is assumed. Mathematically we can express it as

$$P(C \mid IM = x) = \Theta\left[\frac{\ln\left(\dfrac{x}{\theta}\right)}{\beta}\right] \tag{1}$$

where $P(C \mid IM = x)$ represents the probability that a ground motion with $IM = x$ shall cause the structure to reach the specified DM, $\Theta()$ is the standard normal cumulative distribution function (CDF), $\theta$ and $\beta$ respectively are median of the fitted function (IM level for 50% probability of meeting a specified LS) and standard deviation of lnIM. To determine the parameters $\theta$ and $\beta$, method of moment estimator is used when IDA is adopted to collect information of structural response. Further details of these procedures are available in the literature (Baker and Eerri 2014). Among others, Güneyisi and Nazl (2014) have shown the usefulness of seismic fragility to understand the performance of viscoelastically damped system) relative to traditional moment-resisting frames.

The following section describes a straightforward extension of IDA procedure from one-component shaking to two-component shaking. Although this extension is not essentially new, the present study rationalizes as to how the ground motion should be intensified pair-wise. Further, the issue of selection of appropriate IM along with the procedure of combing the component intensities to represent a bi-directional shaking is essentially crucial. These have been addressed in the present work.

## 3. IDA under two-component shaking

In standard IDA under uni-directional shaking, a structure is subjected to a ground motion with increasing intensity. Increasing intensity is achieved by factorizing the component (up and down) to achieve desired response. Standard response history analysis in each step is conducted to evaluate structural demand corresponding to multiple levels of intensity. To extend this traditional IDA to account for bi-directional interaction, we have proposed the following:

• The structure is analyzed by subjecting it to a pair of horizontal component applied along two principal axes of the structure. Ground motion components are intensified by multiplying each component by a constant factor.

• IM of the motion pair-wise applied on the structure is expressed as the geometric mean of the component IMs.

• In each step of analysis, we have combined the displacement time series (not independent peaks component-wise) in each principal direction by SRSS rule and maximum over the history is taken as the demand under bi-directional excitation.

The considerations described above need justification. We propose to amplify both the components of a record by identical factor since this does not distort the relative amplitude of the components. Relative amplitude of the components is an important aspect to regulate structural response under bi-directional shaking (Sengupta *et al*. 2016). It may, however, be contended that the scaling of ground motion is seismologically deficient since intensifying motion corresponds to an event of greater magnitude that results in change of spectral shape or frequency content. This is a well-known limitation of IDA even when conducted under uni-directional shaking (Grigoriu 2011, Banerjee *et al*. 2016). Conversely, standard IDA may be viewed as analyzing structures with a range of capacity in order to choose one that satisfies the design aims under a target event. Thus the standard IDA appears meaningful, both under uni-directional and bi-directional shaking, interpreting IDA as a means to estimate the characteristics of appropriate structure yielding an intended demand under a specified earthquake. For such interpretation only, standard IDA is acceptable and applying identical scale factor to both the components of motion is admissible. The deficiency of scaling the motion, regardless of whether IDA is applied under one or two components, may otherwise be eliminated by a conceptually sound Multiple Stripe Analysis (MSA) (Banerjee *et al*. 2016) using real records in the as-recorded form. While the method may appear to be computationally challenging in view of collecting many accelerograms with appropriate intensities, effect of bi-directional shaking may be accounted for in the same line.

We represent geometric mean (GM) of IMs of two horizontal components as the measure of the combined intensity of motion. Beyond the fact that this is traditionally used, we may refer to the earlier works (Bazzurro *et al*. 2006, Lucchini *et al*. 2011), where GM of IMs have been noted to be efficient. In fact, a comparison with other combinations does not appear to reveal any significant difference.

We now conduct IDA on a single storey structure under eleven NF and eleven FF records. IDA curves under both uni-directional and bi-directional shaking are established. Subsequently, fragility is established and the efficiency of alternative IMs is examined.

## 4. Constructing fragility per IDA under two-component shaking

### 4.1 Structural idealization

The current investigation selects a single storey nominally symmetric building frame with rigid diaphragm (refer to Banerjee *et al*. 2016). Mass of the building lumped at the diaphragm is adjusted to achieve fundamental period (T) of vibration of structure as 0.2 sec, 1.0 sec and 3.0 sec respectively. The following sections outline the considerations adopted in the modelling of the structure.

Present investigation models building columns using distributed plasticity. Force-based

formulations is adopted, while discretizing the member cross-section into fibres. The sectional moment-curvature state is then obtained through the integration of the nonlinear uniaxial stress-strain response of each fiber. The global inelasticity of the member is subsequently achieved by integration of the contribution of each controlling section (Gauss section). Column cross-section is discretized into two hundred fibers with four Gauss sections. Gauss-Lobatto quadrature rule is used to numerically integrate the forced-based elements (Alemdar and White 2005).

Uni-axial stress-strain model for reinforced concrete, initially proposed by Mander *et al.* (1988) and improved subsequently by Martinez-Rueda and Elnashai (1997) has been used. Typical section consists of unconfined concrete (40 mm cover), confined concrete and reinforcing steel. Characteristic strength of concrete and strain at peak stress are respectively taken as 30 MPa and 0.28%. Confinement effect due to lateral reinforcement is taken into account through the definition of the confinement factor of section core (Mander et al.1988) chosen as 1.5. Thus, the loss of member strength due to spalling of concrete cover is accounted. It is assumed that once ultimate conditions are reached, RC members continue to have a residual strength (Mpampatsikos *et al.* 2008). Mander *et al.* (1988) model has also been adopted in another recent work to parametrically explore seismic fragility of RC buildings (Nagashree *et al.* 2016).

Constitutive behavior for reinforcement steel (Yield strength 415 MPa and Elastic modulus $2 \times 10^5$ MPa) is modeled using Menegotto-Pinto steel model (Menegotto and Pinto 1973) modified by Filippou *et al.* (1983). This model assumes a bilinear backbone curve with isotropic strain hardening (1.5%). The model takes into account the *Bauschinger* effect. This idealization has been implemented in standard software SeismoStruct V.6 (2004). Similar modelling has recently been used in other studies (Sengupta *et al.* 2016, Banerjee *et al.* 2016).

### 4.2 Ground motions

Ground motions consequent to an earthquake reflect the features of the seismic source, the rupture process, the travel path from source to site and local site conditions. Selection of appropriate records is, therefore, very crucial consistent with a design scenario primarily regulated by magnitude-distance-soil condition triads (Elnashai and Di Sarno 2010). It is well-known that the representation of a design scenario is more closely related to the proximity of magnitude rather than distance (Elnashai and Di Sarno 2010).

It is well-known that the characteristics of ground motion in the vicinity of an active fault can be significantly different from that of the far-field. Thus, the seismic excitations used in the present investigation consists of near-fault (NF) and far-fault (FF) motions. Near-fault (NF) ground motions often contain strong long-period pulse in the acceleration history that appears as coherent pulse in the velocity and displacement histories (Singh 1985, Somerville *et al.* 1997, Somerville 2003). Such a pronounced pulse does not exist in motions recorded at far-fault region (Chopra 2008). This clearly distinguishes them from typical far-fault motions. One of the most damaging potential of NF accelerograms is forward directivity (FD). This occurs when the rupture front propagates toward the site and the direction of slip on the fault is aligned with the site.

Thus the ground motions compiled herein from PEER strong motion database (http://peer.berkeley.edu) includes two sub-sets each comprising eleven accelerograms. The first set (Table 1(a)) is representative of near-fault motions with forward directive signature, while the far-fault motions are grouped in the second (Table 1(b)). The moment magnitude ($M_w$) and closest site-to-fault-rupture distance (R) for the NF accelerograms ranges from 5.7 to 6.9 and from 4.0 km

to 12.9 km, respectively. These parameters for FF motions vary from 6.2 to 7.3 and from 17.6 km to 42.0 km, respectively. Average shear wave velocity in the top 30 meters of the site ($V_s30$) is also included in Table 1.

Table 1(a) Details of near-fault ground motions

| Sl. No | Event (date of occurrence)[1] | Station | Component Identifier | Vs30 (m/s) | Fault type | $M_w$ | R (km) |
|---|---|---|---|---|---|---|---|
| 1 | Chalfant Valley-01 07/20/86 | Zack Brothers Ranch | NGA_no_547_B-ZAK360 | 271 | SS | 5.8 | 6.4 |
| | | | NGA_no_547_B-ZAK270 | | | | |
| 2 | Coyote Lake 08/06/79 | Gilroy Array #3 | NGA_no_148_G03140 | 350 | SS | 5.7 | 7.4 |
| | | | NGA_no_148_G03050 | | | | |
| 3 | Dinar, Turkey 01/10/95 | Dinar | NGA_no_1141_DIN180 | 220 | N | 6.4 | 3.4 |
| | | | NGA_no_1141_DIN090 | | | | |
| 4 | Imperial Valley-06 10/15/79 | EL Centro Array #3 | NGA_no_178_H-E03230 | 163 | SS | 6.5 | 12.9 |
| | | | NGA_no_178_H-E03140 | | | | |
| 5 | Imperial Valley-06 10/15/79 | EL Centro Array #5 | NGA_no_180_H-E05230 | 206 | SS | 6.5 | 4.0 |
| | | | NGA_no_180_H-E05140 | | | | |
| 6 | Imperial Valley-06 10/15/79 | SAHOP Casa Flores | NGA_no_189_H-SHP270 | 339 | SS | 6.5 | 9.6 |
| | | | NGA_no_189_H-SHP000 | | | | |
| 7 | Loma Prieta 10/18/89 | Saratoga – Aloha Ave | NGA_no_802_STG090 | 371 | RV-OBL | 6.9 | 8.5 |
| | | | NGA_no_802_STG000 | | | | |
| 8 | Mammoth Lakes-01 05/25/80 | Convict Creek | NGA_no_230_I-CVK180 | 339 | N-OBL | 6.1 | 6.6 |
| | | | NGA_no_230_I-CVK090 | | | | |
| 9 | Morgan Hill 04/24/84 | Halls Valley | NGA_no_461_HVR240 | 282 | SS | 6.2 | 3.5 |
| | | | NGA_no_461_HVR150 | | | | |
| 10 | Northridge-01 01/17/94 | Sun Valley – Roscoe Blvd | NGA_no_1082_RO3090 | 309 | RV | 6.7 | 10.1 |
| | | | NGA_no_1082_RO3000 | | | | |
| 11 | Westmorland 04/26/81 | Westmorland Fire Sta. | NGA_no_319_WSM180 | 194 | SS | 5.9 | 6.5 |
| | | | NGA_no_319_WSM090 | | | | |

**\*1 : mm/dd/yy**
$M_w$ - Moment magnitude, **R** - closest site-to-fault-rupture distance, **Vs30** – Shear wave velocity, **SS** – Strike slip, **RV** – Reverse, **RV-OBL** – Reverse oblique, **N** – Normal, **N-OBL** – Normal oblique

## 4.3 Results and discussions

Variation of inter-storey drift (DM) for all reference structures with different periods is computed under all NF and FF records per conventional IDA till global instability, dictated by the robust numerical model, is attained. This is performed by repeating standard response history analysis under chosen accelerograms scaling at multiple levels of intensity. IDA is conducted both under uni-directional and bi-directional shaking for each event. Response history analysis is conducted in the time domain using Hilber-Hughes-Taylor integration scheme (Hilber *et al.* 1977). Hilber-Hughes-Taylor parameters α, γ and β are chosen respectively as -0.1, 0.6 and 0.3025 with sufficiently small time step of integration to ensure convergence. 5% of critical damping and displacement/ rotation based criterion (tolerance limits: 0.1mm and $10^{-4}$ rad) for convergence are employed. This is implemented in the framework of standard software Seismo-Struct – V: 6.

Table 1(b) Details of far-fault ground motions

| Sl. No | Event (date of occurrence)[1] | Station | Component Identifier | Vs30 (m/s) | Fault type | $M_w$ | R (km) |
|---|---|---|---|---|---|---|---|
| 1 | Cape Mendocino 04/25/92 | Eureka-Myrtle and West | NGA_no_826_EUR090 | 457 | RV | 7.0 | 20.0 |
| | | | NGA_no_826_EUR000 | | | | |
| 2 | Cape Mendocino 04/25/92 | Fortuna—Fortuna Blvd | NGA_no_827_FOR090 | 345 | SS | 7.3 | 21.8 |
| | | | NGA_no_827_FOR000 | | | | |
| 3 | Landers 06/28/92 | Desert Hot Springs | NGA_no_850_DSP090 | 207 | SS | 7.3 | 36.2 |
| | | | NGA_no_850_DSP000 | | | | |
| 4 | Landers 06/28/92 | Palm Springs Airport | NGA_no_884_PSA090 | 354 | SS | 7.3 | 23.6 |
| | | | NGA_no_884_PSA000 | | | | |
| 5 | Landers 06/28/92 | Yermo Fire Station | NGA_no_900_YER360 | 133 | RV-OBL | 6.9 | 43.2 |
| | | | NGA_no_900_YER270 | | | | |
| 6 | Loma Prieta 10/18/89 | APEEL 2—Redwood City | NGA_no_732_A02133 | 425 | RV | 6.7 | 35.8 |
| | | | NGA_no_732_A02043 | | | | |
| 7 | Northridge-01 01/17/94 | Lake Hughes #1 | NGA_no_1019_L01090 | 425 | RV | 6.6 | 27.4 |
| | | | NGA_no_1019_L01000 | | | | |
| 8 | San Fernando 02/09/71 | Lake Hughes #1 | NGA_no_70_L01111 | 453 | RV | 6.6 | 29.0 |
| | | | NGA_no_70_L01021 | | | | |
| 9 | San Fernando 02/09/71 | Palmdale Fire Station | NGA_no_78_PDL210 | 299 | RV | 6.6 | 39.5 |
| | | | NGA_no_78_PDL120 | | | | |
| 10 | San Fernando 02/09/71 | Whittier Narrows Dam | NGA_no_93_WND233 | 207 | SS | 6.2 | 17.6 |
| | | | NGA_no_93_WND143 | | | | |
| 11 | Superstition Hills-01 11/24/87 | Wildlife Liquef. Array | NGA_no_718_A-IVW360 | 194 | SS | 5.9 | 6.5 |
| | | | NGA_no_718_A-IVW090 | | | | |

**[1] : mm/dd/yy**

$M_w$ - Moment magnitude, **R** - closest site-to-fault-rupture distance, **Vs30** – Shear wave velocity, **SS** – Strike slip, **RV** – Reverse, **RV-OBL** – Reverse oblique, **N** – Normal, **N-OBL** – Normal oblique

*Debdulal Pramanik, Abhik Kumar Banerjee and Rana Roy*
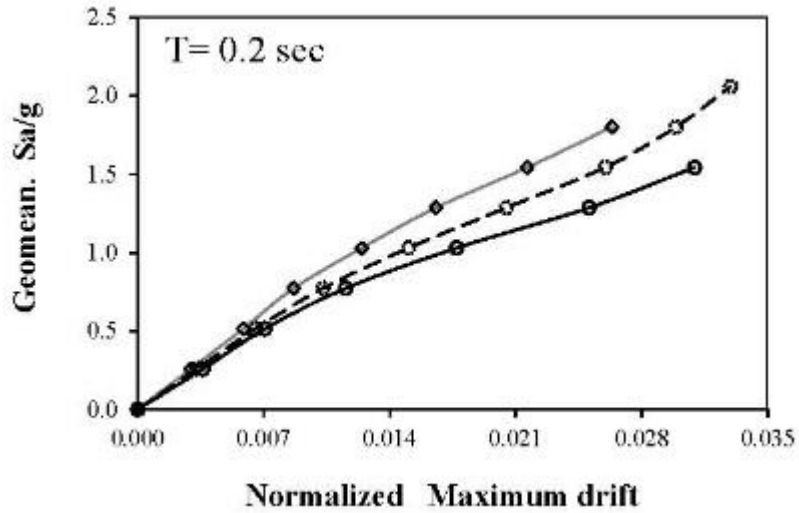


(a) Event: Chalfant Valley-01, 07/20/86, Station: Zack Brothers Ranch (NF)
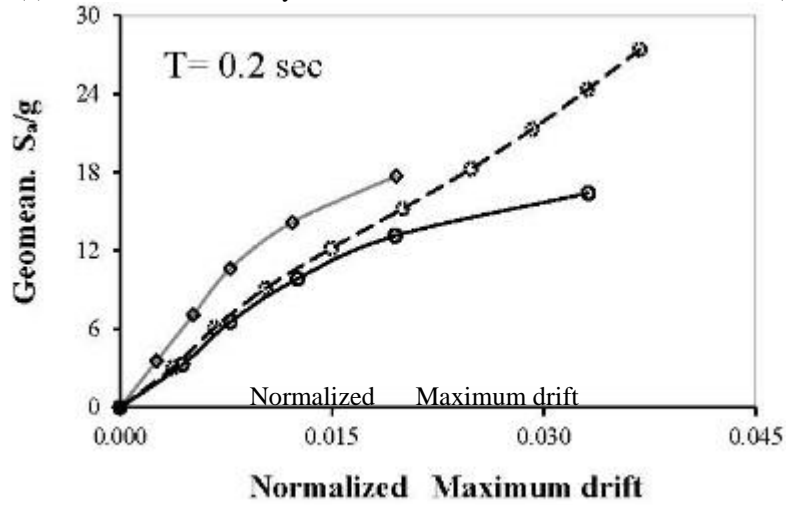


(b) Event: Cape Mendocino 04/25/92, Station: Eureka-Myrtle and West (FF)

◇———— Unidirectional shaking

—✧— — Unidirectional shaking (considered in fragility)

○———— Bidirectional shaking

Fig. 1 Construction of seismic fragility under bi-directional shaking

GM of IM is taken to represent the shaking level even in case of uni-directional analysis as the true accelerogram involves both the components and analysis under uni-directional shaking is a mathematical simplification of the real scenario. IDA curves corresponding to each component response so constructed are compared pair-wise. IDA curve that yields greater DM at a relatively lower value of IM is considered as IDA curve due to uni-directional shaking (refer to Fig. 1 for sample presentation).
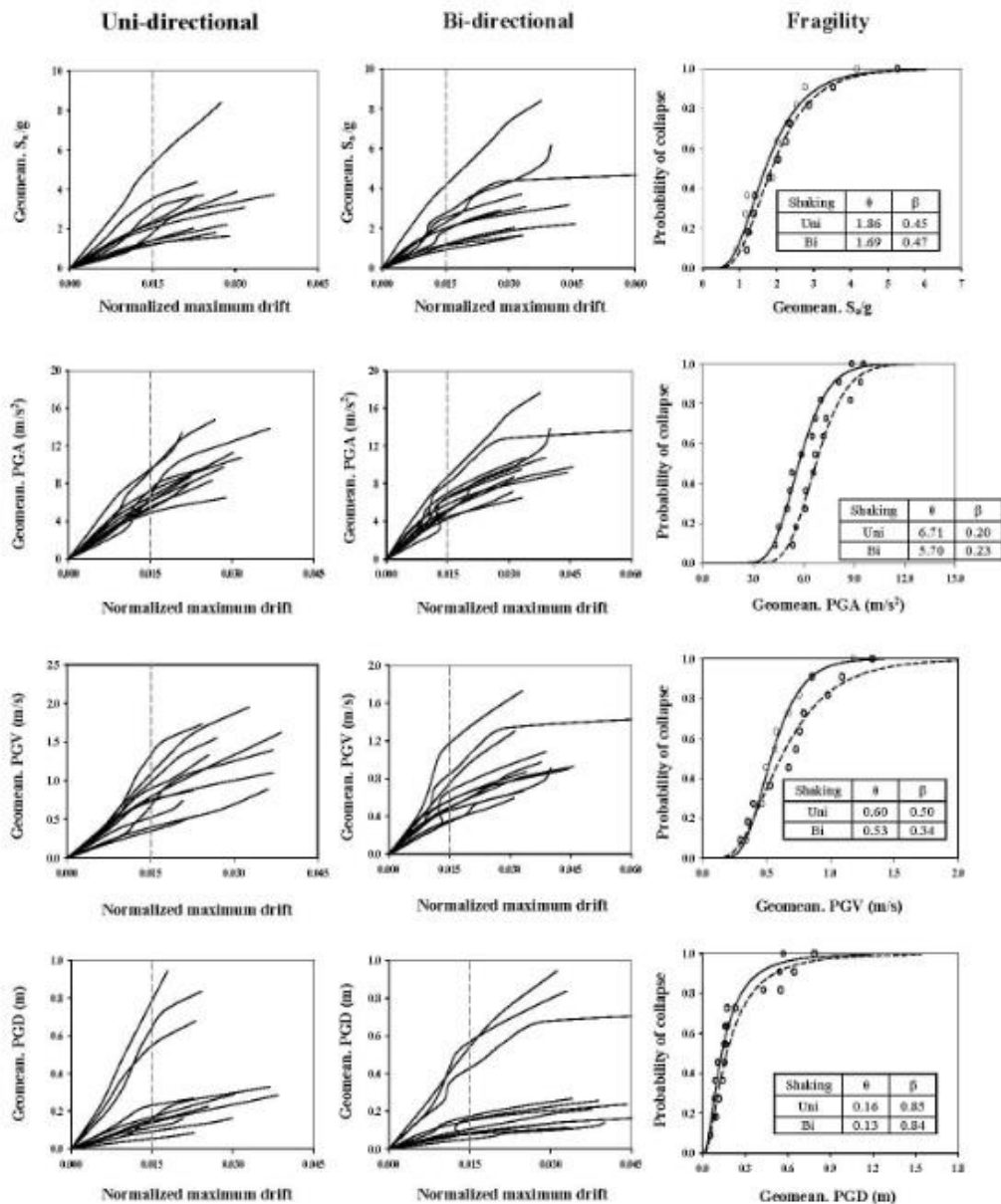


Fig. 2(a) Seismic structural fragility under near-fault excitation (T= 0.2sec)

IDA is constructed under eleven NF and eleven FF records and for all reference systems under uni-directional and bi-directional shaking. Results so obtained are presented in the form of standard IDA curves as a function different alternative IMs in Fig. 2 under NF motions. Variation of similar demand parameter with corresponding IM, as obtained from uni-directional and bi-directional analysis, is furnished alongside. Seismic fragility curves corresponding to a displacement demand of 1.5% i.e., upper limit for damage control limit state (Banerjee *et al.* 2016) are constructed on the basis of the response statistics from IDA. Parameters measuring median ($\theta$) and dispersion of lnIM ($\beta$) associated with the seismic fragility fitted is summarized in each case.
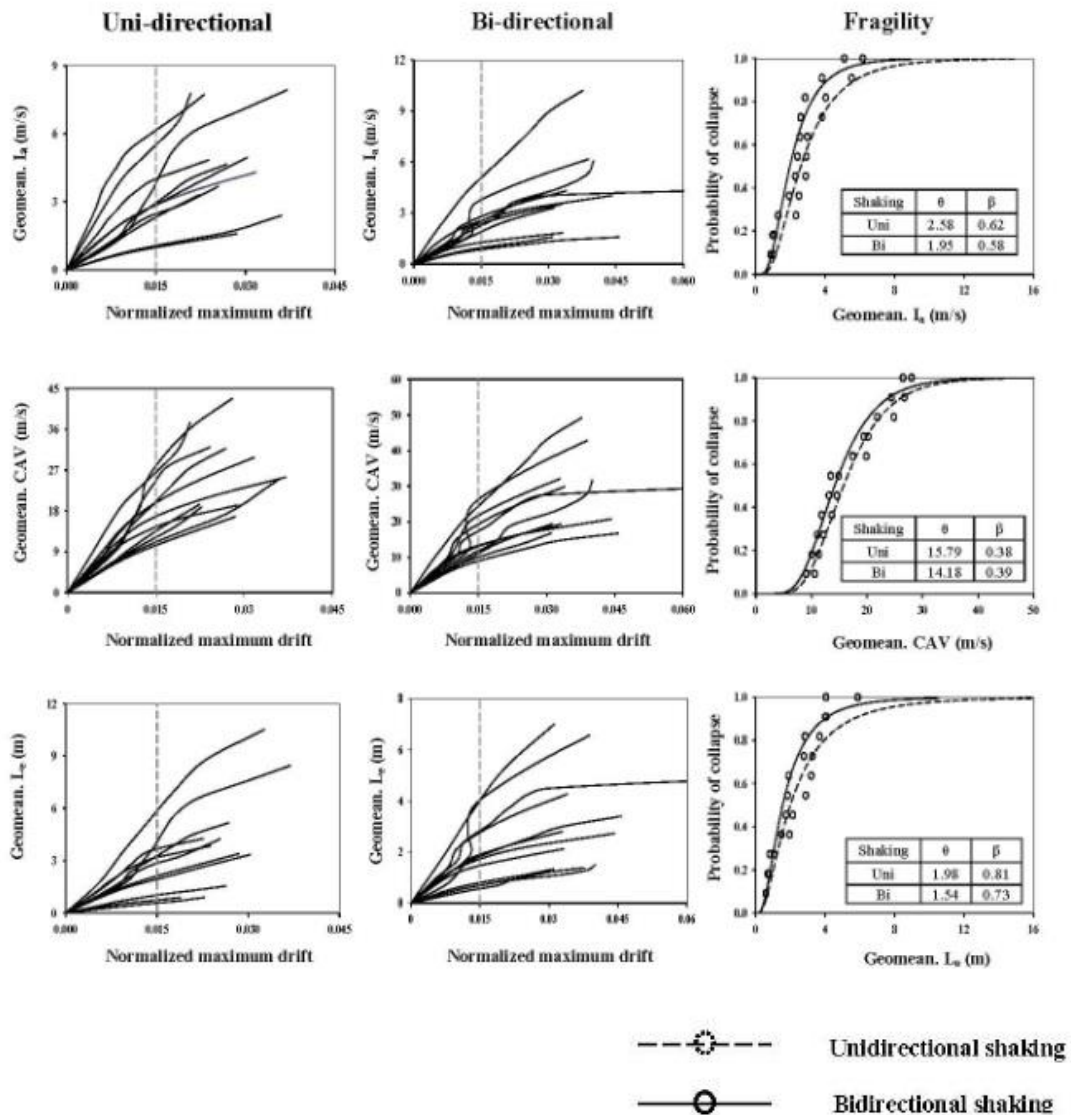


Fig. 2 (contd.): Seismic structural fragility under near-fault excitation (T= 0.2 sec)
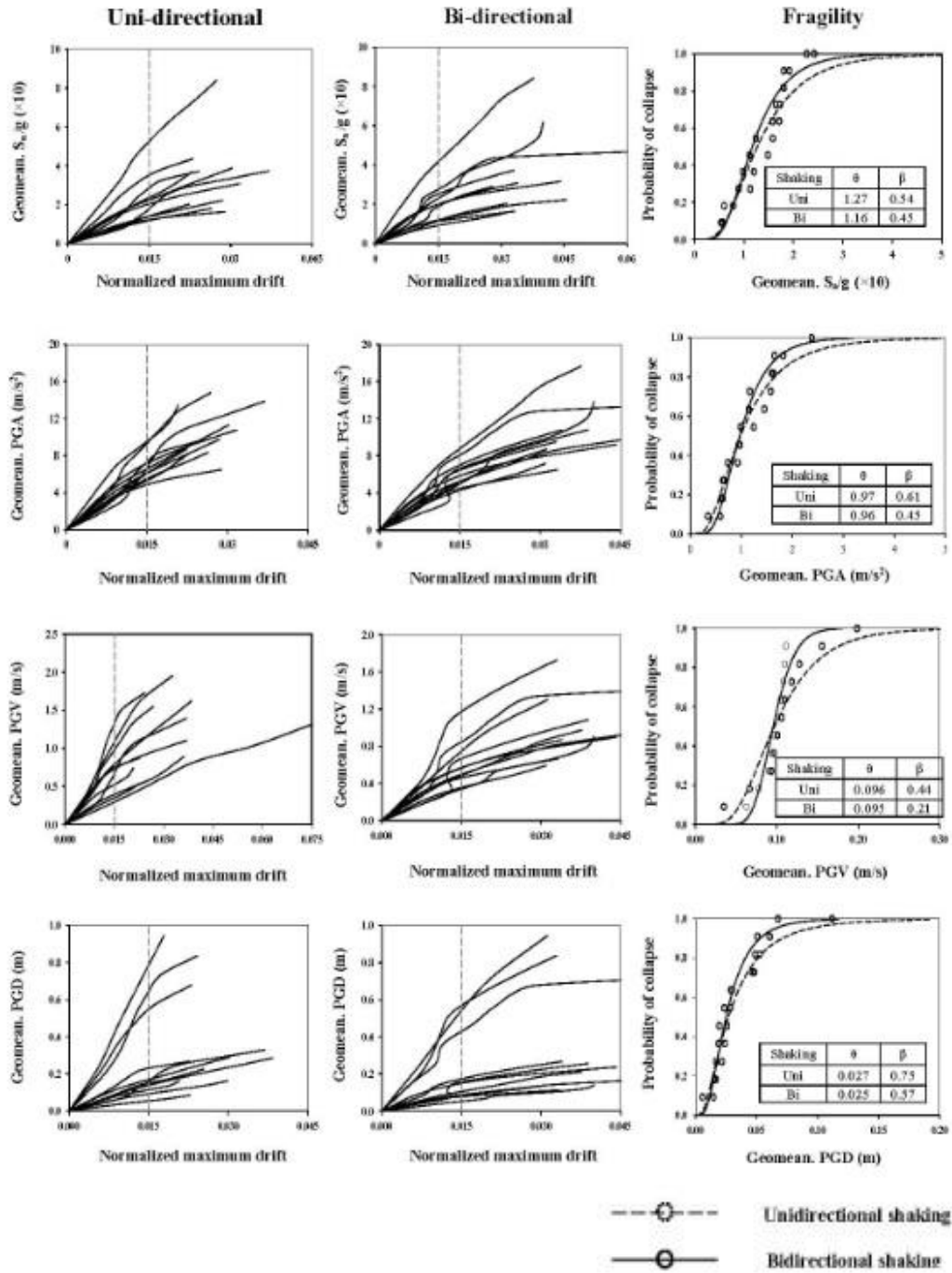
Fig. 2(b) Seismic structural fragility under near-fault excitation (T = 1.0sec)
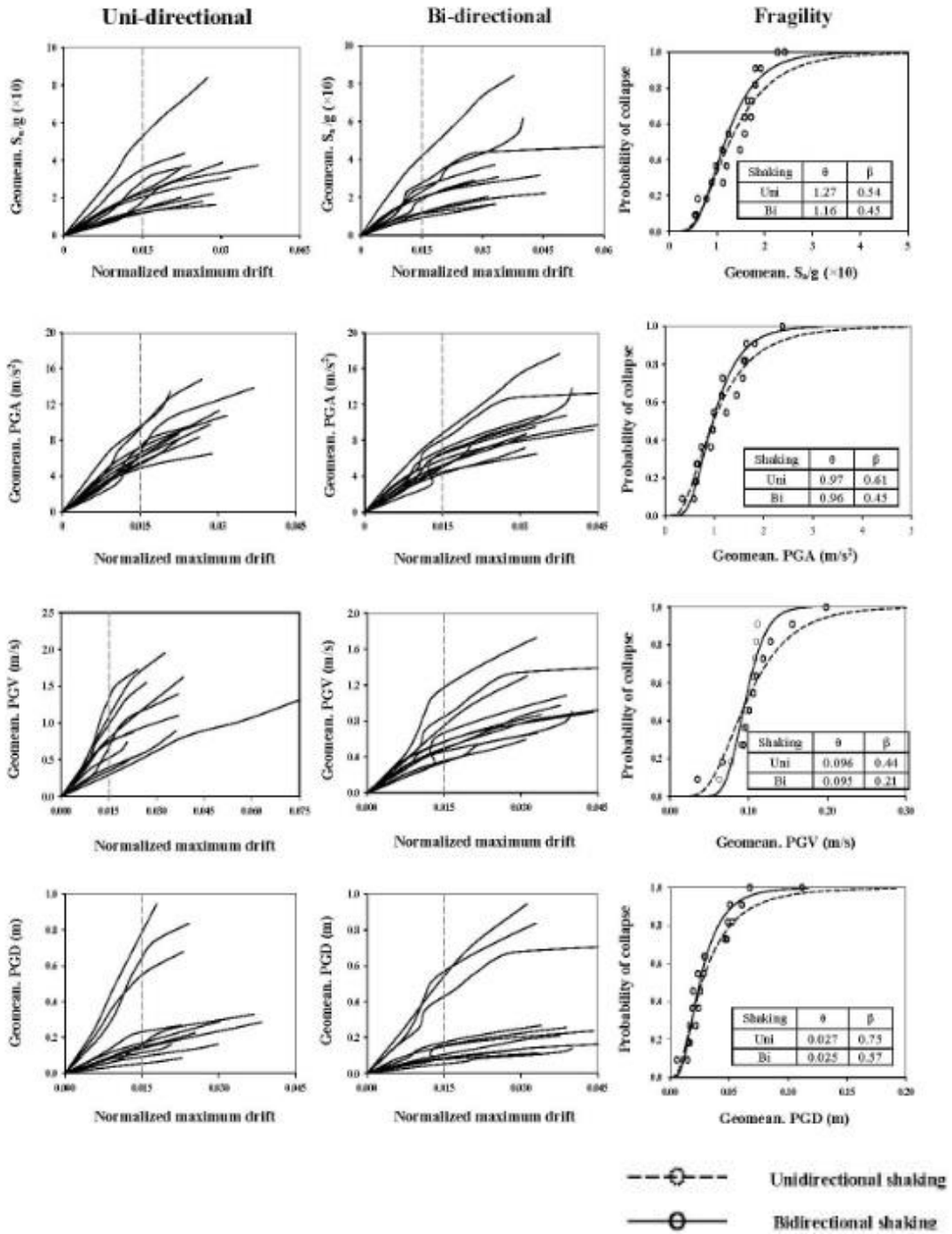
Fig. 2(b) (contd): Seismic structural fragility under near-fault excitation (T = 1.0 sec.)
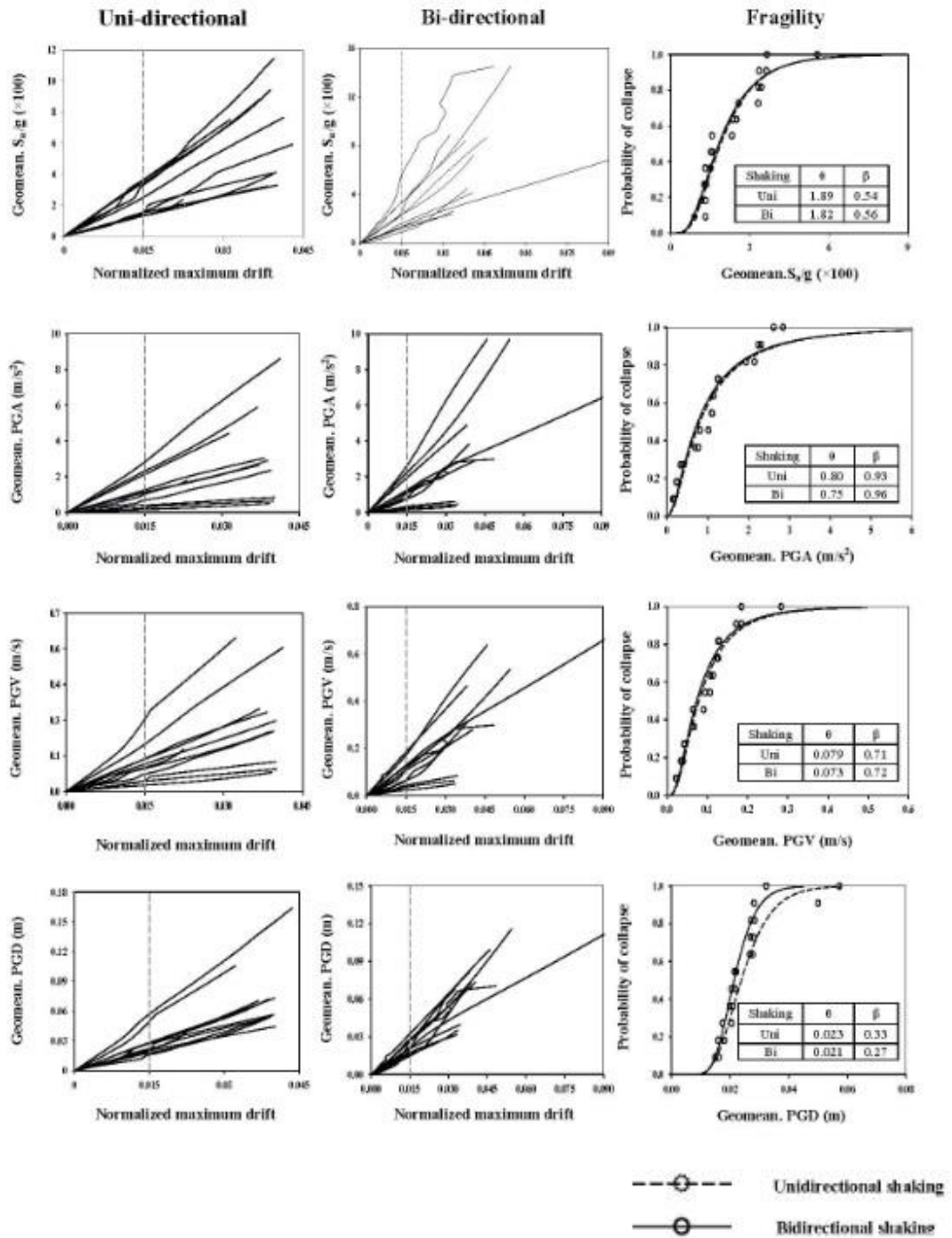
Fig. 2 (c) Seismic structural fragility under near-fault excitation (T = 3.0 sec.)

| | Uni-directional | Bi-directional | Fragility |
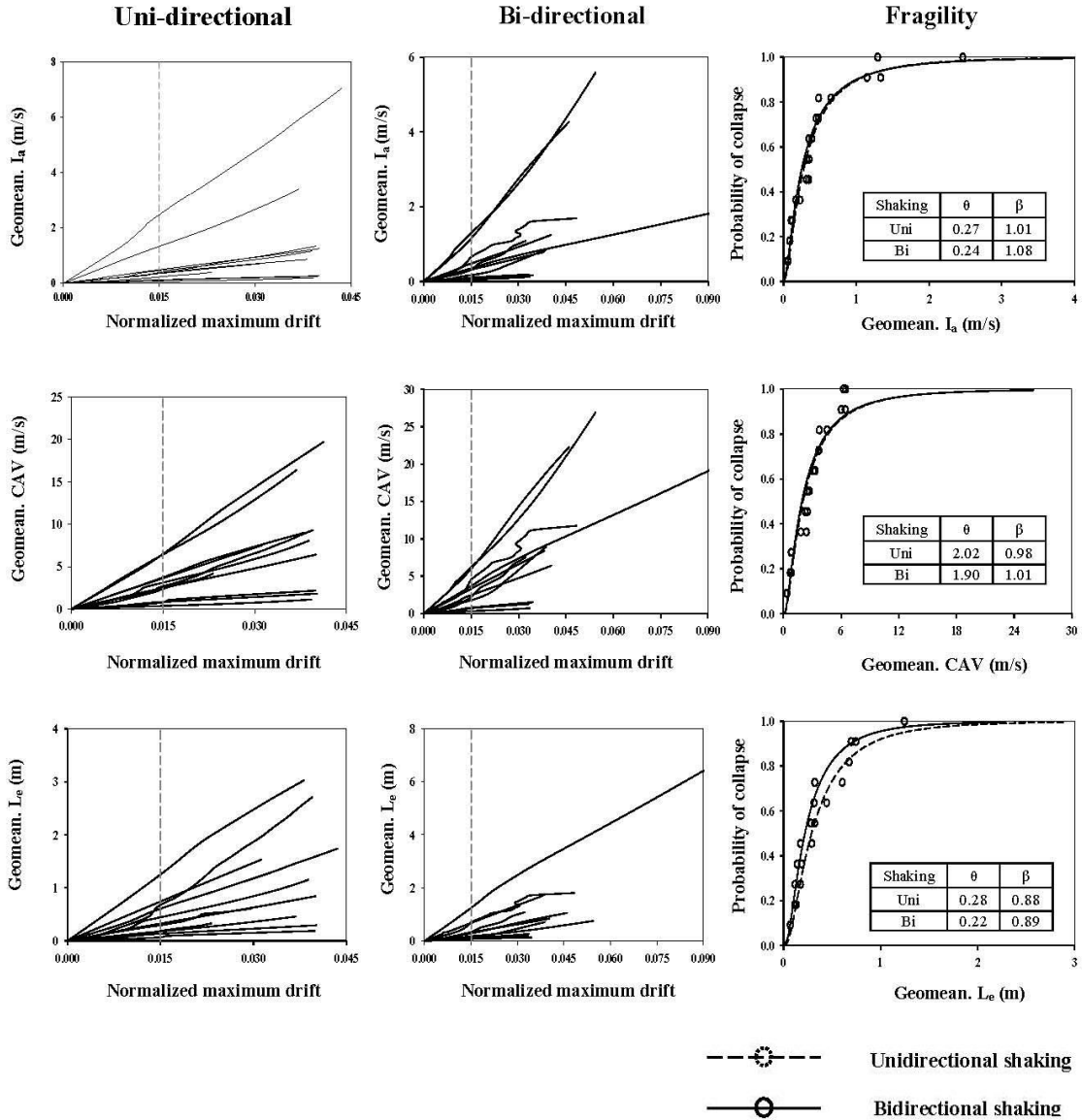


Fig. 2(c) (contd): Seismic structural fragility under near-fault excitation (T = 3.0 sec.)

IDA curves under uni-directional and bi-directional shaking as well as the fragility estimates are presented for a set of selected IMs, *viz.*, $S_a$, PGA, PGV, PGD, $I_a$, CAV, $L_e$ respectively through Fig. 2(a) for system with period equals to 0.2 sec. under NF excitations. Similar variation is presented in Figs. 2(b) and 2(c) for systems with periods 1.0 sec. and 3.0 sec. under NF motions. Values of θ and β for these systems with periods 0.2 sec., 1.0 sec. and 3.0 sec. are further summarized in Table 2 for ready comparison. It is evident that the estimated dispersion as reflected

through β is sensitive to the selected IM. Careful scrutiny further indicates that this β becomes minimum for the choice of PGA, PGV and PGD as reference IM respectively for systems with period equals to 0.2 sec., 1.0 sec. and 3.0 sec. (highlighted in the tables). In this context, standard response spectrum plotted in tripartite format may be referred. This suggests that structural response is more directly associated with PGA, PGV and PGD for systems in short, medium and long period regimes, respectively (Chopra 2008). The relative efficiency of PGA, PGV and PGD respectively in short, medium and long period regimes may be a direct consequence of the same. It may be restated that a chosen IM is considered efficient if the variance of the same at any performance state as may be measured through β is small. It is generally expected that β should be within 0.20 – 0.30 to hold a proper efficiency, while the same with even around 0.40 are 'reasonably acceptable' (Mollaioli *et al.* 2013). Response presented in Fig. 3 under FF excitations and the relevant summary of β in Table 3 also corroborates this inferences. It may further be noticed from Figs. 2 and 3 that the fragility curves under uni-directional and bi-directional shaking are relatively close. This is also reflected through the relatively close values of θ (refer to Tables 2 and 3) estimated for uni-directional and bi-directional shaking. Significance of bi-directional shaking, however, appears pronounced for short period systems.

Table 2 Values of θ and β of fitted fragility function for near-fault motions. U and B respectively correspond to cases due to uni-directional and bi-directional shaking

| IM | θ | | | β | |
|---|---|---|---|---|---|
| | U | B | % of Change | U | B |
| **T = 0.2 s** | | | | | |
| $S_a/g$ | 1.86 | 1.69 | -9.13 | 0.45 | 0.47 |
| **PGA (m/s$^2$)** | 6.71 | 5.70 | **-15.05** | **0.20** | **0.23** |
| PGV (m/s) | 0.60 | 0.53 | -11.66 | 0.50 | 0.34 |
| PGD (m) | 0.16 | 0.13 | -18.75 | 0.85 | 0.84 |
| AI (m/s) | 2.58 | 1.95 | -24.41 | 0.62 | 0.58 |
| CAV (m/s) | 15.79 | 14.18 | -10.19 | 0.38 | 0.39 |
| $L_e$ (m) | 1.98 | 1.54 | -22.22 | 0.81 | 0.73 |
| **T = 1.0 s** | | | | | |
| $S_a/g(\times 10)$ | 1.270 | 1.160 | -8.66 | 0.54 | 0.45 |
| PGA (m/s$^2$) | 0.970 | 0.960 | -1.03 | 0.61 | 0.45 |
| **PGV (m/s)** | 0.096 | 0.095 | **-1.04** | **0.44** | **0.21** |
| PGD (m) | 0.027 | 0.025 | -7.40 | 0.75 | 0.57 |
| AI (m/s) | 0.320 | 0.330 | 3.12 | 0.70 | 0.48 |
| CAV (m/s) | 2.280 | 2.440 | 7.01 | 0.49 | 0.39 |
| Le (m) | 0.360 | 0.310 | -13.88 | 0.81 | 0.58 |
| **T = 3.0 s** | | | | | |
| $S_a/g(\times 100)$ | 1.890 | 1.820 | -3.70 | 0.54 | 0.56 |
| PGA (m/s$^2$) | 0.800 | 0.750 | -6.25 | 0.93 | 0.96 |
| PGV (m/s) | 0.079 | 0.073 | -7.59 | 0.71 | 0.72 |
| **PGD (m)** | 0.023 | 0.021 | **-8.69** | **0.33** | **0.27** |
| AI (m/s) | 0.270 | 0.240 | -11.11 | 1.01 | 1.08 |
| CAV (m/s) | 2.020 | 1.900 | -5.94 | 0.98 | 1.01 |
| Le (m) | 0.280 | 0.220 | -21.42 | 0.88 | 0.89 |
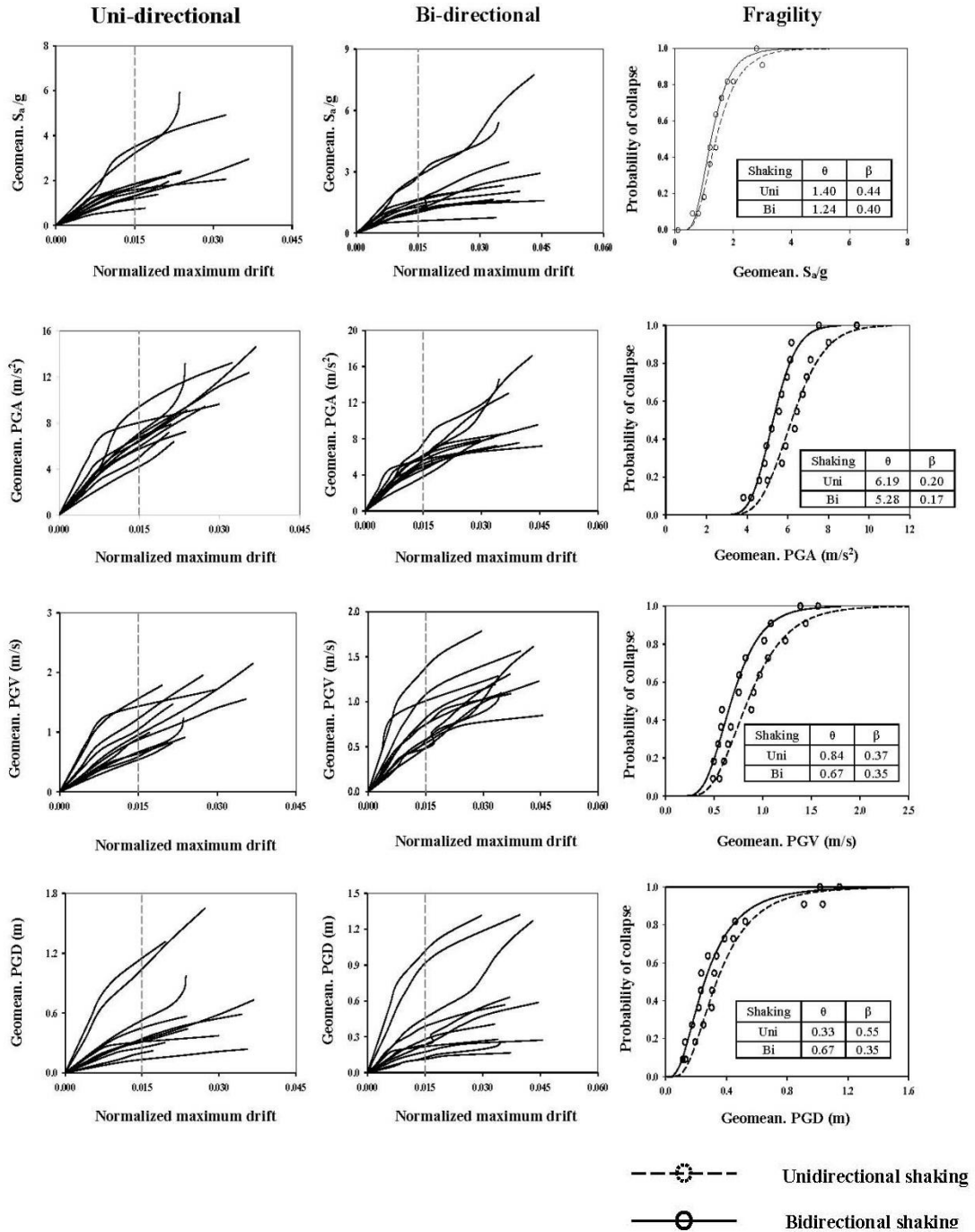
Fig. 3(a) Seismic structural fragility under far-fault excitation (T = 0.2 sec.)

## 5. Implications of combination rules

It is thus apparent that the phenomenon of seismic bi-lateral interaction may be important for stiff systems for which PGA is an effective IM. It is, therefore, interesting to check the adequacy of combination rules, viz., '30%', '40%' to predict bi-directional response from two separate uni-directional analyses under two horizontal components of accelerogram. To this end, response under bi-directional shaking using uni-directional responses ($r_{(C)}$) has been computed by combination rules as under:

$$r_{(c)} = \text{max. of } [1.0r_x + \gamma r_y, 1.0r_y + \gamma r_x] \qquad (2)$$

where $r_x$, $r_y$ are peak responses under two components of motion uni-directionally and separately applied along two principal axes of the structure, $\gamma$ is 0.3 or 0.4 in '30%' and '40%' respectively. Seismic fragilities for system with T = 0.2 sec. are furnished in Fig. 4. This shows that the '30% rule' may be effectively used to account for the bi-directional interaction. Currently, AASHTO 1998 recommends '30% rule' to estimate response under bi-directional shaking per uni-directional analysis. Thus the present study asserts the current views of the modern codes available worldwide.

Table 3 Values of θ and β of fitted fragility function for far-fault motions. U and B respectively correspond to cases due to uni-directional and bi-directional shaking

| IM | θ | | | β | |
|---|---|---|---|---|---|
| | U | B | % of Change | U | B |
| **T = 0.2 s** | | | | | |
| $S_a/g$ | 1.40 | 1.24 | -11.42 | 0.44 | 0.40 |
| **PGA (m/s²)** | 6.19 | 5.28 | **-14.70** | **0.20** | **0.17** |
| PGV (m/s) | 0.84 | 0.67 | -20.23 | 0.37 | 0.35 |
| PGD (m) | 0.33 | 0.67 | 103.03 | 0.55 | 0.35 |
| AI (m/s) | 1.47 | 1.20 | -18.36 | 0.48 | 0.47 |
| CAV (m/s) | 25.37 | 21.46 | -15.41 | 0.21 | 0.23 |
| $L_e$ (m) | 2.88 | 2.42 | -15.97 | 0.64 | 0.63 |
| **T = 1.0 s** | | | | | |
| $S_a/g(\times10)$ | 1.230 | 1.250 | 1.62 | 0.93 | 0.72 |
| PGA (m/s²) | 0.670 | 0.580 | -13.43 | 0.41 | 0.47 |
| **PGV (m/s)** | 0.087 | 0.078 | **-11.36** | **0.39** | **0.45** |
| PGD (m) | 0.037 | 0.029 | -21.62 | 0.73 | 0.7 |
| AI (m/s) | 0.150 | 0.130 | -13.33 | 0.45 | 0.56 |
| CAV (m/s) | 2.700 | 2.540 | -5.92 | 0.43 | 0.51 |
| Le (m) | 0.370 | 0.280 | -24.32 | 0.45 | 0.36 |
| **T = 3.0 s** | | | | | |
| $S_a/g(\times100)$ | 2.010 | 1.730 | -13.93 | 0.75 | 0.69 |
| PGA (m/s²) | 0.380 | 0.400 | 5.26 | 0.68 | 0.89 |
| PGV (m/s) | 0.057 | 0.055 | -3.50 | 0.60 | 0.71 |
| **PGD (m)** | 0.026 | 0.023 | **-11.53** | **0.18** | **0.20** |
| AI (m/s) | 0.098 | 0.099 | 1.02 | 0.76 | 0.92 |
| CAV (m/s) | 1.780 | 1.840 | 3.37 | 0.76 | 0.79 |
| Le (m) | 0.220 | 0.200 | -9.09 | 0.86 | 0.93 |
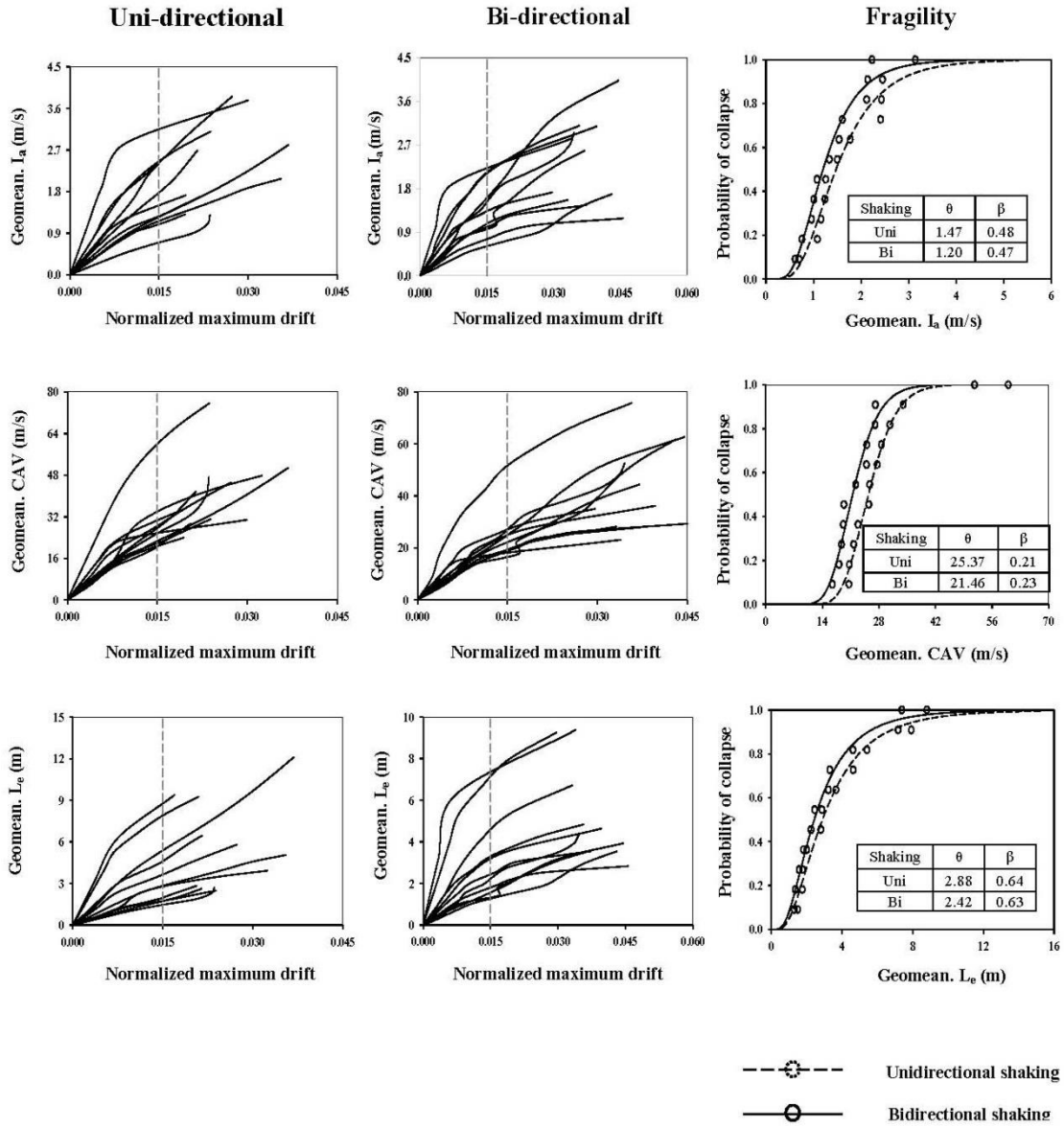
Fig. 3(a) (contd) Seismic structural fragility under far-fault excitation (T = 0.2 sec)
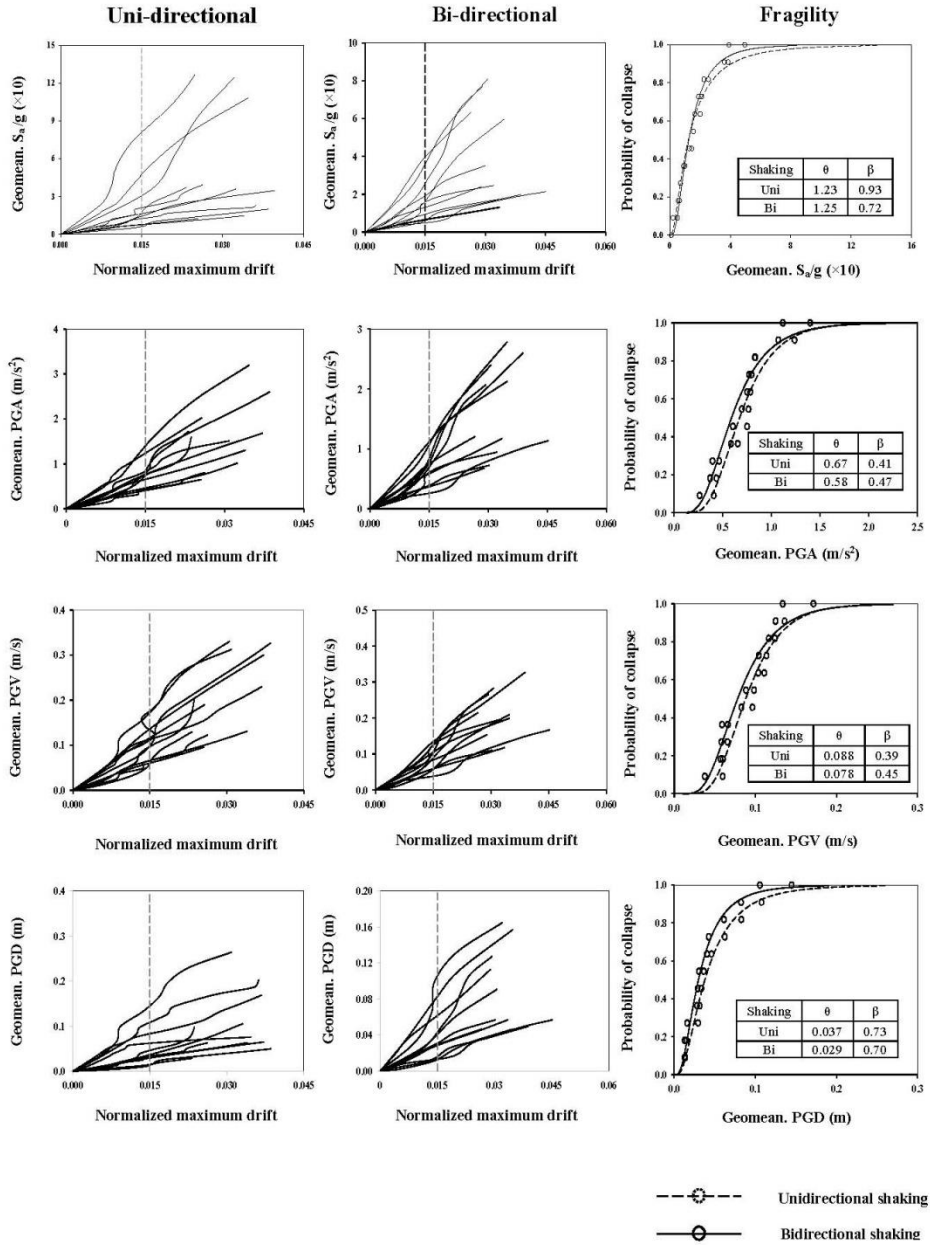
Fig. 3(b) Seismic structural fragility under far-fault excitation (T = 1.0 sec.)
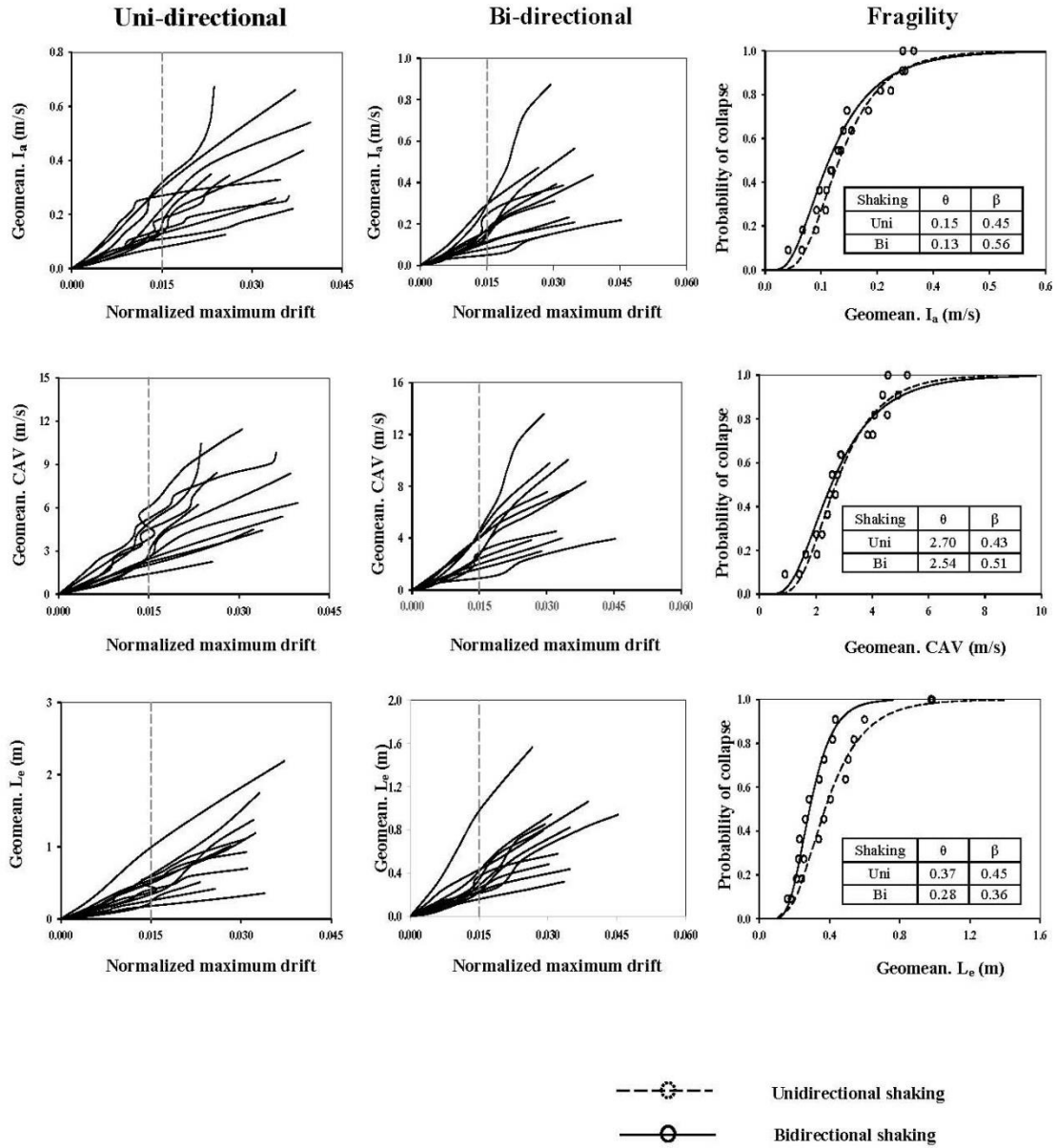
Fig. 3(b) (contd): Seismic structural fragility under far-fault excitation (T = 1.0 sec.)
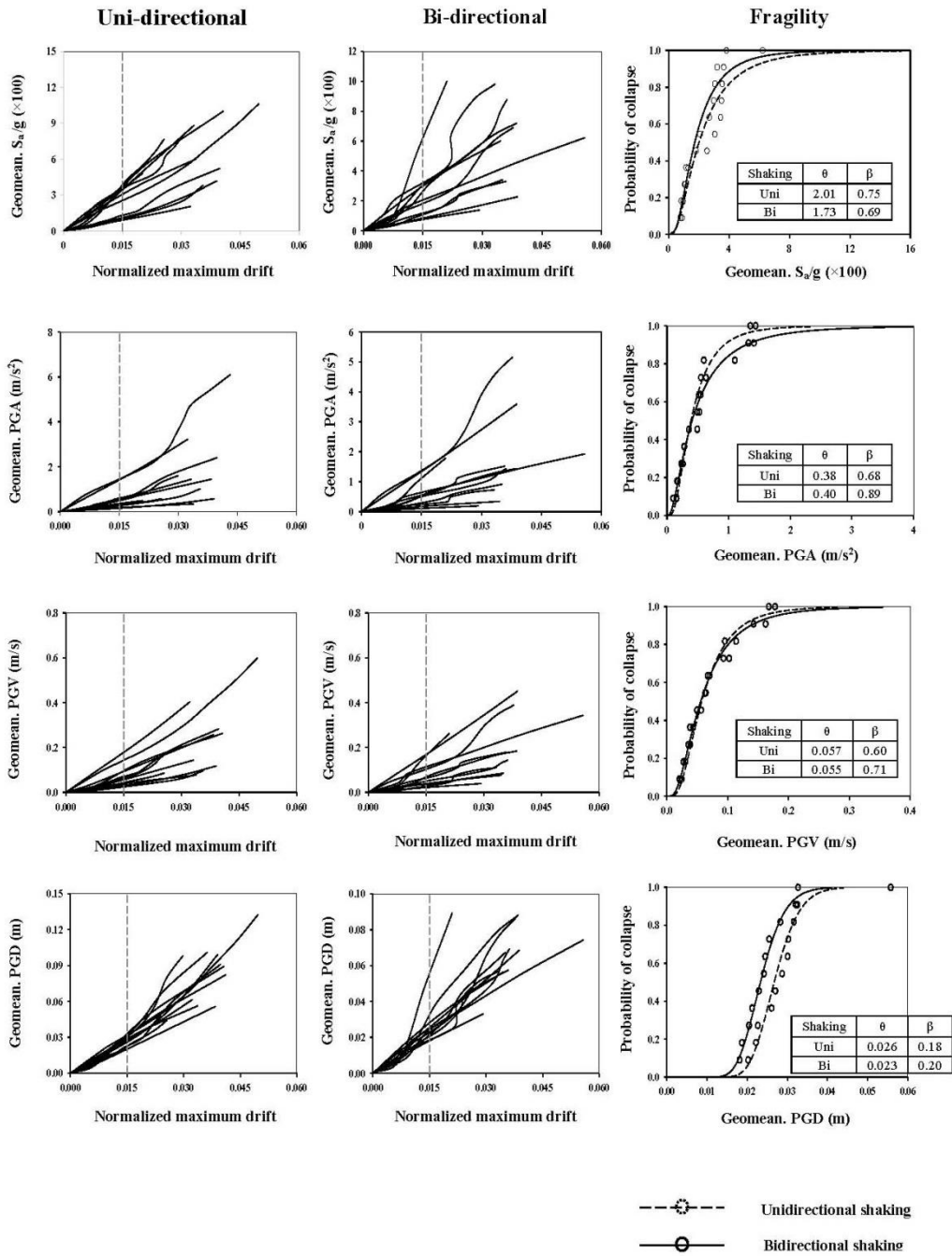
Fig. 3(c) Seismic structural fragility under far-fault excitation (T = 3.0 sec.)
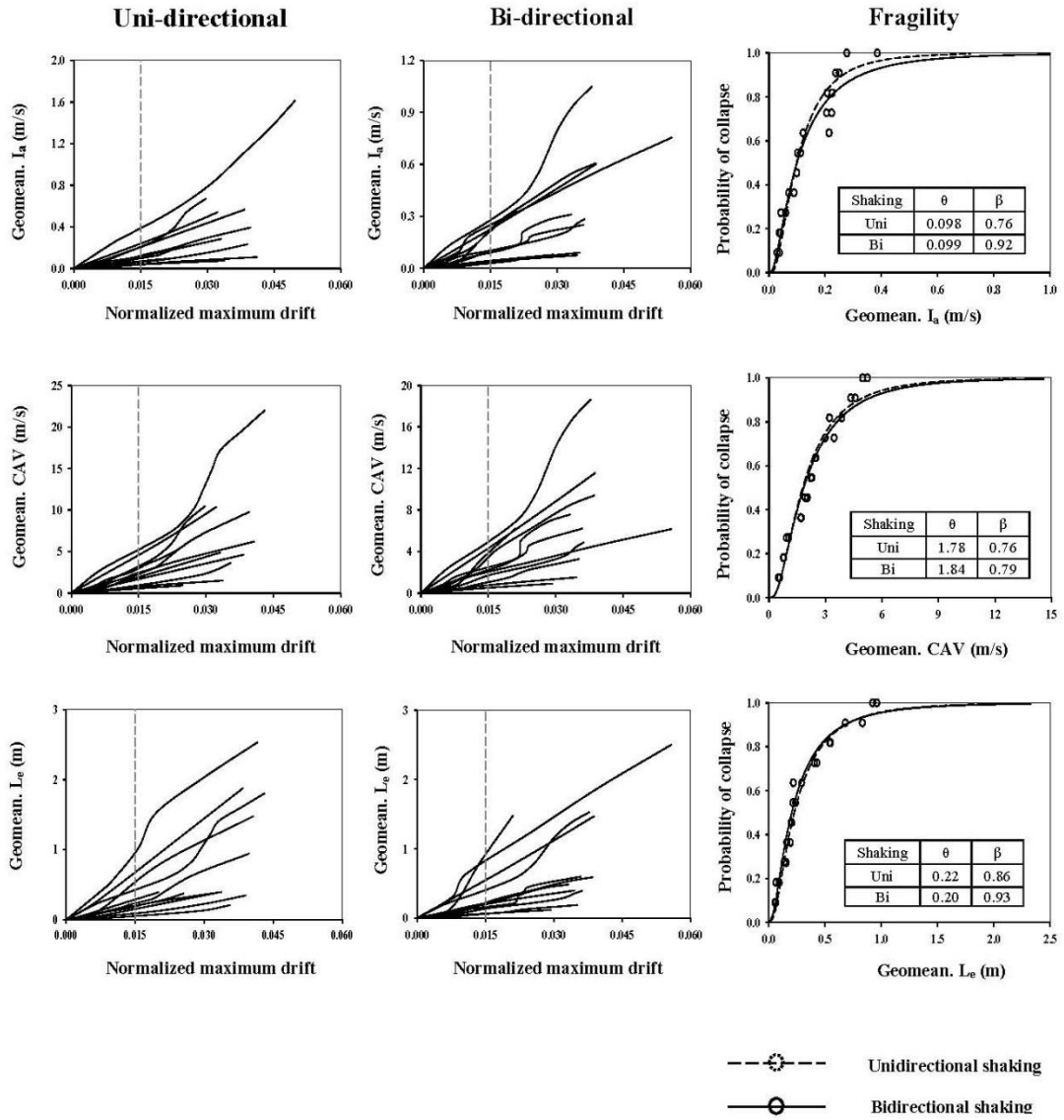
Fig. 3(c) (contd): Seismic structural fragility under far-fault excitation (T = 3.0 sec.)
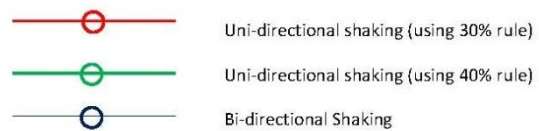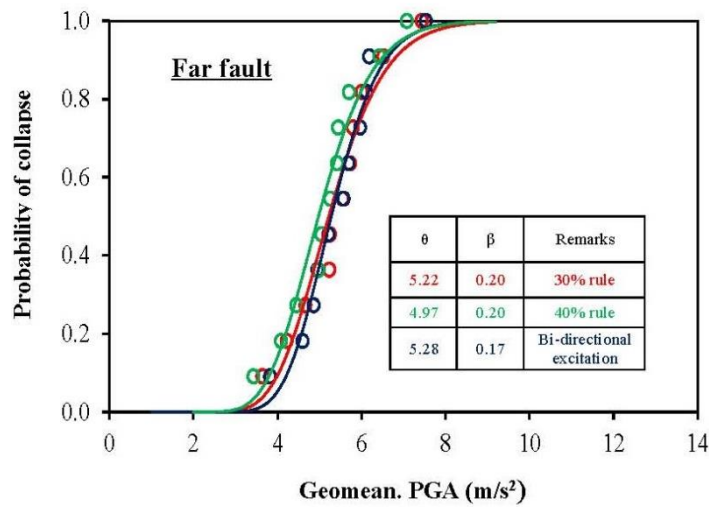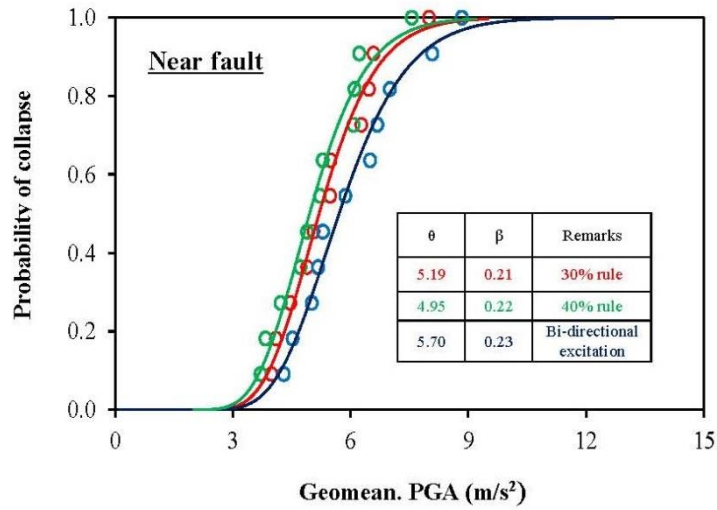
Fig. 4 Adequacy of codified combination rules to predict seismic structural fragility under near-fault and far-fault excitations (T = 0.2 sec.)

## 6. Conclusions

Current design generally evaluates inelastic seismic demand under bi-directional shaking through combining responses under uni-directional excitation using simple rule. Seismic fragility is often estimated by assessing structural response from IDA. Further, controversies do exist regarding the suitability of the IMs that may be used in these methods. In this backdrop, seismic fragility in terms of different IMs is estimated using simple structural models with different periods. Structure is subjected to uni-directional and bi-directional shaking employing a set of NF and FF motions with increasing intensity. Results may be summarized to the following broad conclusions.

1. The present study estimates seismic fragilities accounting for bi-directional interaction. The logical extension of conventional IDA under uni-directional shaking to prepare IDA curves to represent real bi-directional loading scenario may appear useful. Geometric mean of the component intensities is considered as IM of real event.
2. Selection of appropriate IM is often a very critical issue for the construction of IDA curves. The present study resolves that the geometric mean of two horizontal components' PGA, PGV and PGD may be selected as effective IM for systems with short, medium and long period systems respectively. Efficacy of the IMs, however, awaits further investigation in the framework of the procedure emerged in the present study with more number of accelerograms.
3. Codified combination rules (viz., 30%) to predict bi-directional response from two separate uni-directional analyses may be considered adequate to establish seismic fragilities for short period systems.

Conclusions above are generally applicable under both NF and FF excitations. The present study is conducted using equivalent single storey system with different periods. The conclusions of this study should, therefore, be re-examined for systems that include participation of higher modes. Such study, to arrive at a more stable unbiased assessment on the efficacy of the proposed IMs, should involve more number of accelerograms.

## References

Alemdar, B.N. and White, D.W. (2005). "Displacement, flexibility and mixed beam- column finite element formulations for distributed plasticity analysis", *J. Struct. Eng. - ASCE*, **131**(12), 1811-1819.
American Association of State Highway and Transportation Officials (AASHTO) (1998), *LRFD Bridge Design Specification*, 2nd Ed., AASHTO, Washington, D.C.
Baker, J.W. and Eerri, M. (2014), "Efficient analytical fragility function fitting using dynamic structural analysis", Technical Note, *Earthquake Spectra*, **23**(2), 471-489.
Banerjee, A.K., Pramanik, D. and Roy, R. (2016), "Seismic structural fragilities: proposals for improved methodology per spectral matching of accelerogram", *Eng. Struct.*, **111**, 538-515.
Bazzurro, P., Park, J. and Tothong, P. (2006), "Multidirectional seismic excitation effects in building response estimation", Collaborative Research with USGS and AIR.
Bertero, V.V. (1977), "Strength and deformation capacities of buildings under extreme environments", *Structural Engineering and Structural Mechanics*, (Ed., K. S. Pister), Prentice Hall, Englewood Cliffs, NJ.
Beyer, K. and Bommer, J.J. (2007), "Selection and scaling of real accelerogram directional loading: A review of current practice and code provisions", *J. Earthq. Eng.*, **11**, 13-45.
Bradley, B.A. and Dhakal, R.P. (2008), "Error estimation of closed-form solution for annual rate of structural collapse", *Earthq. Eng. Struct. D.*, **37**(15), 1721-1737.
Chakroborty, S. and Roy, R. (2016), "Role of ground motion characteristics on inelastic seismic response of

irregular structures", *J. Architect. Eng. - ASCE*, **22**(1), B4015003, 1-16.

Chopra, A.K. (2008), "Dynamics of Structures", Prentice Hall Private Limited, New Jersey, USA.

Eads, L., Miranda, E., Krawinkler, H. and Lignos, D.G. (2013), "An efficient method for estimating the collapse risk of structures in seismic regions", *Earthq. Eng. Struct. D.*, **42**(1), 25-41.

Ebrahimian, H., Jaleyer, F., Lucchini, A. and Manfredi, G. (2015), "Preliminary ranking of alternative scalar and vector intensity measures of ground shaking", *Bulletin of Earthquake Engineering.*

Elnashai, A.S. and Di Sarno, L. (2010), "Fundamentals of earthquake engineering", John Wiley & sons Ltd, West Sussex, United Kingdom.

Filippou, F.C., Popov, E.P. and Bertero, V.V. (1983), "Effects of bond deterioration on hysteretic behaviour of reinforced concrete joints", Report EERC **83-19**, Earthquake Engineering Research Center, University of California, Berkeley.

Ghafory-Ashtiany, M., Mousavi, M. and Azarbakht, A. (2010), "Strong ground motion record selection for the reliable prediction of the mean seismic collapse capacity of a structure group", *Earthq. Eng. Struct. D.*, **40**(6), 691-708.

Grigoriu, M. (2011), "To scale or not to scale seismic ground-acceleration records", *J. Eng. Mech. - ASCE*, **137**(4), 284-293.

Güneyisi, E.M. and Sahin, N.D. (2014), "Seismic fragility analysis of conventional and viscoelastically damped moment resisting frames", *Earthq. Struct.*, **7**(3), 295-316.

Hachem, M.M., Mahin, S.A. and Moehle, J.P. (2003), "Performance of circular reinforced concrete bridge columns under bi-directional earthquake loading", Pacific Earthquake Engineering Research Centre, Report No. PEER **2003/06**.

IS 1893 (2002), Criteria for Earthquake Resistant Design of Structures, Part 1: General Provisions and Buildings.

Kitajima, K., Adachi, H. and Nakanishi, M. (1996), "Response characteristics of reinforced concrete structures under bi-directional earthquake motions", *Proceedings of the 11th World Conference on Earthquake Engineering*, Pergamon, Elsevier Science Ltd., Oxford, England, Disc 1, Paper No. **566**.

Kitajima, K., Koizumi, T., Akiyama, H., Kanda, M., Nakanishi, M. and Adachi, H. (1992), "Response characteristics of reinforced concrete columns under bi-directional earthquake motions", *Proceedings of the 10th World Conference on Earthquake Engineering*.

Kubo, T. and Penzien, J. (1979), "Analysis of three-dimensional strong ground motions along principal axes, San Fernando Earthquake", *Earthq. Eng. Struct. D.*, **7**(3), 265-278.

Lucchini, A., Mollaioli, F. and Monti, G. (2011), "Intensity measures for response prediction of a torsional building subjected to bi-directional earthquake ground motion", *Bull. Earthq. Eng.*, **9**, 1499-1518.

Mander, J.B., Priestley, M.J.N. and Park, R. (1988), "Theoretical stress–strain model for confined concrete", *J. Struct. Eng. - ASCE*, **114**(8), 1804-1823.

Martinez-Rueda, J.E. and Elnashai, A.S. (1997), "Confined concrete model under cyclic load", *Mater. Struct.*, **30**(197), 139-147.

Menegotto M. and Pinto P.E. (1973), "Method of analysis for cyclically loaded R.C. plane frames including changes in geometry and non-elastic behaviour of elements under combined normal force and bending", *Symposium on the Resistance and Ultimate Deformability of Structures Acted on by Well Defined Repeated Loads*, International Association for Bridge and Structural Engineering, Zurich, Switzerland, 15-22.

Moehle, J.P. and Deierlein, G.G. (2004), "A framework methodology for performance-based earthquake engineering", *Proceedings of the 13th world conference on earthquake engineering*, Vancouver, Canada, 1-6, August.

Mollaioli, F., Lucchini, A., Cheng Y. and Monti, G., (2013), "Intensity measures for the seismic response prediction of base-isolated buildings", *Bull. Earthq. Eng.,* **11**(5), 1841-1866.

Mpampatsikos, V., Nascimbene, R. and Petrini, L. (2008), "A critical review of the R.C. frame existing building assessment procedure according to Eurocode 8 and Italian Seismic Code", *J. Earthq. Eng,*, **12**(1), 52-58.

Nagashree, B.K., Ravi Kumar, C.M. and Venkat Reddy, D. (2016), "A parametric study on seismic fragility analysis of RC buildings", *Earthq. Struct.*, **10**(3), 629-643.

Nakayama, T. *et al.* (1996), "Shaking table tests of reinforced concrete structures under bidirectional earthquake motions", *Proceedings of the 11th World Conference on Earthquake Engineering*, Oxford, England, Paper No. **1001**.

Nassar, A.A. and Krawinkler, H. (1991), "Seismic demands for SDOF and MDOF systems", Report No. **95**, The John A.Blume Earthquake Engineering Center, Stanford University, Stanford, CA.

Porter, K., Kennedy, R. and Bachman, R. (2007), "Creating Fragility Functions for performance-Based Earthquake Engineering", *Earthq. Spectra*, **23**(2), 471-489.

Rathje, E.M., Abrahamson, N.A. and Bray, J.D. (1998), "Simplified frequency content estimates of earthquake ground motions", *J. Geotech. Eng.- ASCE*, **124**(2), 150-159.

Rathje, E.M., Faraj, F., Russell, S. and Bray, J.D. (2004), "Empirical relationships for frequency content parameters of earthquake ground motions", *Earthq. Spectra*, **20**(1), 119-144.

Roy, R., Ghosh, D. and Bhattcharaya, G. (2015), "Influence of strong motion characteristics on permanent displacement of slopes", *Landslides*, **13**(2), 279-292.

SeismoSoft (2013), "SeismoStruct V. 6 - A computer program for static and dynamic nonlinear analysis of framed structures [online]", ed: available from URL: http://www.seismosoft.com.

Sengupta, A., Quadery, L., Sarkar, S. and Roy, R. (2016), "Influence of bi-directional near-fault excitations on RC bridge piers", *J. Bridge Eng. - ASCE* , **21**(7), 04016034: 1-3.

Singh, J.P. (1985). "Earthquake ground motions: Implications for designing structures and reconciling structural damage", *Earthq. Spectra,* **1**(2), 239-270.

Somerville, P.G. (2003), "Magnitude scaling of the near fault rupture directivity pulse", *J. Phys. Earth Planetary. Interiors,* **137**(1- 4), 201-212.

Somerville, P.G., Smith, N., Graves, R. and Abrahamson, N. (1997), "Modification of empirical strong ground motion attenuation relations to include the amplitude and duration effects of rupture directivity", *Seismol. Res. Lett.*, **68**(1), 199-222.

Vamvatsikos, D. (2002), "Seismic Performance, Capacity and Reliability of Structures as seen through Incremental Dynamic Analysis", *PhD Thesis*, Stanford University, USA.

Vamvatsikos, D. and Cornell, C.A. (2002a), "Incremental dynamic analysis", *Earthq. Eng. Struct. D.*, **31**(3), 491-514.

Vamvatsikos, D. and Cornell, C.A. (2002b), Tracing and post-processing of IDA curves: Theory and software implementation, Report No. RMS-**44**, RMS Program, Stanford University, Stanford, CA.

Vamvatsikos, D. and Cornell, C.A. (2004b), "Direct estimation of the seismic demand and capacity of MDOF systems through incremental dynamic analysis of an SDOF approximation", *J. Struct. Eng. - ASCE*, **20**(2), 523-553.

Vamvatsikos, D. and Cornell, C.A. (2005), "Developing efficient scalar and vector intensity measures for IDA capacity estimation by incorporating elastic spectral shape information", *Earthq. Eng. Struct. D.*, **34**(13), 1573-1600.

Vamvatsikos, D., and Cornell, C. A. (2004a), "Applied incremental dynamic analysis", *Earthq. Spectra*, **20**(2), 523-553.